Electric Field Comparison of Conventional Transmission Line With Unconventional Transmission Line

Easir Arafat
Zero Emission, Realization of Optimized Energy Systems (ZEROES) Laboratory
Dept. of Electrical and Computer Eng.
The University of Texas at Dallas
Richardson, TX, USA
easir.arafat@utdallas.edu

Babak Porkar
Zero Emission, Realization of Optimized Energy Systems (ZEROES) Laboratory
Dept. of Electrical and Computer Eng.
The University of Texas at Dallas
Richardson, TX, USA
babak.porkar@utdallas.edu

Mona Ghassemi
Zero Emission, Realization of Optimized Energy Systems (ZEROES) Laboratory
Dept. of Electrical and Computer Eng.
The University of Texas at Dallas
Richardson, TX, USA
mona.ghassemi@utdallas.edu

2024 IEEE Texas Power and Energy Conference (TPEC) | 979-8-3503-3120-2/24/$31.00 ©2024 IEEE | DOI: 10.1109/TPEC60005.2024.10472238

***Abstract*—To accommodate the growing demand for electricity, a novel transmission line design has been proposed. This proposed structure must undergo rigorous evaluation to ensure it complies with existing safety standards. As magnetic field and electric field are crucial for the safety of systems and their surroundings, the proposed line must adhere to established limits. This paper presents a comparison of the electric field generated by a newly proposed unconventional overhead line compared to a conventional line where electric field is calculated for each sub-conductor individually. The results demonstrate that the unconventional transmission line exhibits a more favorable electric field profile compared to the conventional line.**

Keywords—Electric field, overhead line, transmission line, extra high voltage, unconventional high surge impedance loading lines.

I. Introduction

To cope with the rising demand for electricity the power industry is expanding constantly. There have been many improvements in generation and distribution systems, such as reducing electric generator sizes, adding renewable energy to the generation sector, and using power electronics to distribute electricity. However, transmission lines have not kept pace with these advancements.

To achieve net-zero emissions in America by 2050, high voltage transmission capacity must expand by approximately 60% by 2030 and triple by 2050. This expansion is necessary to introduce more large-scale solar and wind facilities to the grid, as these renewable energy sources become increasingly important in the fight against climate change. By 2030, an estimated $360 billion will need to be invested in transmission capacity, and $2.4 trillion by 2050 [1].

The deregulation of the U.S. transmission network has made it difficult to efficiently transfer power across open markets and has also led to delays in investment in transmission infrastructure. These delays are due to two main factors: one is the high voltage overhead line owners are more focused on maximizing profits rather than investment in transmission infrastructure and the second one is the complexity of acquiring right-of-way. The increasing focus on renewable energy sources, particularly large-scale solar power plants and wind farms, is elevating the importance of transmission networks. Most of the time, these renewable resources are located far from the destined load centers, necessitating (extra) high voltage (E)HV transmission lines to disperse their generated power.

A major challenge in expanding transmission capacity is the high construction cost for new lines. In 2023, the cost of building a new 500 kV transmission line in the U.S. ranged from $3.9 to $4.8 million per mile [2]. To overcome this challenge, researchers are exploring revolutionary transmission line designs that enhance power transmission density within existing corridors. One approach involves rearranging phase configurations and sub-conductors into optimized geometric structures, leading to increased power delivery capability [3-7].

Conventional methods for calculating electric field intensity on ground level and near ground level are not applicable to these unconventional transmission lines. Existing formulas assume symmetrical sub-conductor arrangements on bundle circles, which is not the case for unconventional lines where sub-conductors can be positioned asymmetrically or at any location in space.

Electric field intensity is a critical parameter in the electrical design of (E)HV transmission lines. It has become more severe when human interaction and other assets face this field. That's why a major concern is to keep it to an acceptable limit when it is time to propose a new EHV overhead line and implement it. In our paper, a method to determine the electric field in the vicinity of the right-of-way for unconventional lines is discussed and the result of this is compared with the conventional one to show the advantage of shifting to the new proposed transmission line.

II. Method

A. Electric Field Calculation

The electric property associated with each point in the space where the charge is present is known as electric field. As power facilities have low frequency and the displacement of charges is very low, it will create electric field around it.

This work was supported in part by the National Science Foundation (NSF) under Award #2306098.

979-8-3503-3120-2/24/$31.00 ©2024 IEEE

To determine the electric field intensity at a certain point P (y, z) shown in Fig. 1 in the surroundings of a transmission line, we need to consider two components:

$$\vec{E} = \{\vec{E}_y, \vec{E}_z\} \tag{1}$$

For the transmission line, we have

$$[q] = [P]^{-1}.[U] \tag{2}$$

where $[U]$ indicates the line to ground voltage phasor matrix, $[q]$ is a matrix of charge, and [P] indicates the matrix of Maxwell potential coefficients. These potential coefficients are calculated in two groups, one is mutual elements and the other is self elements. For an overhead transmission line consisting n parallel conductors, the elements are given by Eqs. (3) and (4).

$$P_{ii} = \frac{1}{2\,\pi\varepsilon_o} \ln \frac{2\,h_i}{R_i} \tag{3}$$

$$P_{ij} = \frac{1}{2\,\pi\varepsilon_o} \ln \frac{D_{ij}}{d_{ij}} \tag{4}$$

where ε_o indicates the dielectric constant of air, h_i indicates the vertical coordinate of the i-th conductor, R_i indicates radius of i-th conductor, d_{ij} indicates the shortest distance between the i and j conductors and D_{ij} indicates the shortest distance between i-th conductor and the image of j-th conductors as represented in Fig. 1.

Now, the components related to the electric field intensity at an arbitrary point introduced by n charges are computed by using the following Eqs. (5) and (6).

$$\vec{E}_y(y,z) = \sum_{i=1}^{n} \frac{q_i}{2\,\pi\varepsilon_o} \left(\frac{y - y_i}{r_i^2} + \Gamma \frac{y - y_i}{r'^2_i} \right) \tag{5}$$

$$\vec{E}_z(y,z) = \sum_{i=1}^{n} \frac{q_i}{2\,\pi\varepsilon_o} \left(\frac{z - z_i}{r_i^2} + \Gamma \frac{z + z_i}{r'^2_i} \right) \tag{6}$$

where (y, z) are arbitrary point coordinates, (y_i, z_i) are charge coordinates, r_i is the shortest distance between the arbitrary point and the i-th point charge, r_i' is the shortest distance between complex image of the i-th point charge and the arbitrary point, as indicated in Fig. 1.

The constant Γ indicates the reflection coefficient which counts the effect of the soil in the case of calculating the electric field at a point. We have considered -1 in our calculations. So, the total electric field at P is.

$$E_{in} = \sqrt{E_{yn}^2 + E_{zn}^2} \tag{7}$$

B. Conventional Overhead Line

In our paper, we have considered a conventional 500 kV transmission line [8] as our base case model with whom we will compare our derived electric field. In Fig. 2, the alignment of its sub-conductors is given.

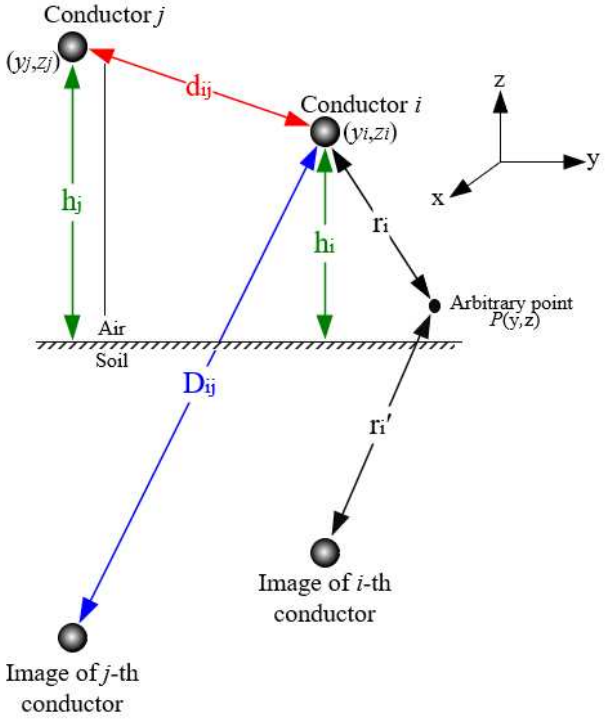

Fig. 1. The distances between the point charges, the image of point charges and an arbitrary point.

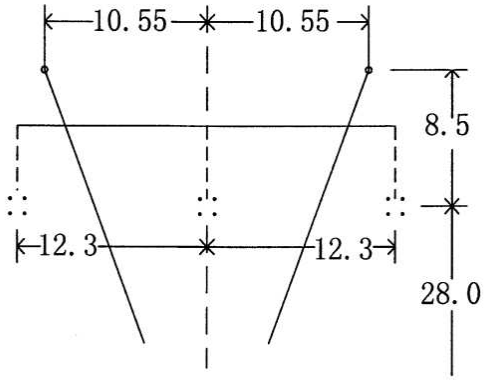

Fig. 2. Phase and the sub-conductor's arrangement of the base case line [8].

The line has a flat phase configuration, with four sub-conductors arranged symmetrically on a circle for each phase. The diameter of each sub-conductor is 26.82 mm and bundle spacing is 45 cm. The phases are 28 meters high. The separation between adjacent phases is 12.3 meters. The resulting natural power for this design is 996.0 MW.

As a three-phase system, three alternating voltages (of the same frequency) are carried by three circuit wires and reach their instantaneous peak levels one-third of a cycle apart. As a single circuit 3-phase line, consider the line voltage as

$$[V] = V_m[\sin(\omega t + \phi), \sin(\omega t + \phi - 120°), \sin(\omega t + \phi + 120°)\ ] \tag{8}$$

Let,

$$J_i = (x - x_i)\left(\frac{1}{r_i^2} - \frac{1}{(r_i')^2}\right) \tag{9}$$

$$K_i = \left(\frac{(y - y_i)}{r_i^2} - \frac{(y + y_i)}{(r_i')^2}\right) \tag{10}$$

Then Eq. (6) will be,

$$E_{v1} = \left(\frac{q_1}{2\pi\epsilon_0}\right) K_1 = V_m.K_1[M_{11}\sin(\omega t + \phi) + M_{12}\sin(\omega t + \phi - 120°) + M_{13}\sin(\omega t + \phi + 120°)] \tag{11}$$

$$E_{v2} = \left(\frac{q_2}{2\pi\epsilon_0}\right) K_2 = V_m.K_2[M_{21}\sin(\omega t + \phi) + M_{22}\sin(\omega t + \phi - 120°) + M_{23}\sin(\omega t + \phi + 120°)] \tag{12}$$

$$E_{v3} = \left(\frac{q_3}{2\pi\epsilon_0}\right) K_3 = V_m.K_3[M_{31}\sin(\omega t + \phi) + M_{32}\sin(\omega t + \phi - 120°) + M_{33}\sin(\omega t + \phi + 120°)] \tag{13}$$

Then total vertical component is

$$\begin{aligned} E_{vn} &= V_m[(K_1 \cdot M_{11} + K_2 \cdot M_{21} + K_3 \cdot M_{31})\sin(\omega t + \phi) \\ &\quad + (K_1 \cdot M_{12} + K_2 \cdot M_{22} + K_3 \cdot M_{32})\sin(\omega t + \phi - 120°) \\ &\quad + (K_1 \cdot M_{13} + K_2 \cdot M_{23} + K_3 \cdot M_{33})\sin(\omega t + \phi + 120°)] \\ &= V_m[K_{v1}\sin(\omega t + \phi) + K_{v2}\sin(\omega t + \phi - 120°) + K_{v3}\sin(\omega t + \phi + 120°)] \end{aligned}$$

and in phasor form,

$$E_{vn} = V_m[K_{v1}\angle\phi + K_{v2}\angle(\phi - 120°) + K_{v3}\angle(\phi + 120°)] \tag{14}$$

Resolving Eq. (14) into real and imaginary parts with $\phi = 0$, we obtain

$$\left.\begin{aligned} real\ part &= K_{v1} - 0.5K_{v2} - 0.5K_{v3} \\ imaginary\ part &= 0 - 0.866K_{v2} + 0.866K_{v3} \end{aligned}\right\} \tag{15}$$

Consequently, the amplitude of electric field is:

$$\begin{aligned} \hat{E}_{vn} &= \sqrt{[(K_{v1} - 0.5K_{v2} - 0.5K_{v3})^2 + 0.75(K_{v3} - K_{v2})^2]} \cdot V_m \\ &= \sqrt{{K_{v1}}^2 + {K_{v2}}^2 + {K_{v3}}^2 - K_{v1}K_{v2} - K_{v2}K_{v3} - K_{v3}K_{v1}} \cdot V_m \\ &= K_v \cdot V_m \end{aligned}$$

The r.m.s. value of the total vertical component at $P(x, y)$ due to all 3 phases will be

$$E_{vn} = \frac{\hat{E}_{vn}}{\sqrt{2}} = K_v \cdot V \tag{16}$$

In a similar manner, the r.m.s. value of a total horizontal component of the field at P due to all 3 phases is

$$\begin{aligned} E_{hn} &= J_h \cdot V \\ &= V.\sqrt{{J_{h1}}^2 + {J_{h2}}^2 + {J_{h3}}^2 - J_{h1}J_{h2} - J_{h2}J_{h3} - J_{h3}J_{h1}} \end{aligned} \tag{17}$$

where,

$$\left.\begin{aligned} J_{h1} &= J_1 \cdot M_{11} + J_2 \cdot M_{21} + J_3 \cdot M_{31} \\ J_{h2} &= J_1 \cdot M_{12} + J_2 \cdot M_{22} + J_3 \cdot M_{32} \\ J_{h3} &= J_1 \cdot M_{13} + J_2 \cdot M_{23} + J_3 \cdot M_{33} \end{aligned}\right\} \tag{18}$$

where the values of J_1, J_2, J_3 are obtained from Eq. (9) for J_i with $i = 1, 2, 3$.

The above equations were coded in MATLAB. For conventional transmission lines, the traditional way is to consider a fictitious conductor instead of bundle conductor. Then the above equation gets a slight change. And the change occurs in Eq. (3), where R_i (radius of the i-th conductor) becomes a_{eq} (equivalent radius). The radius of the fictitious conductor is determined using Eq. (19).

$$a_{eq} = R(N.a/R)^{1/N} \tag{19}$$

R: bundle radius $= B/(2\sin(\pi/N))$ where B: bundle spacing (spacing between adjacent sub-conductors)
N : number of sub-conductors in bundle,
a : radius of each sub-conductor

C. Unconventional Transmission Lines

Our reference to unconventional lines we have considered are two proposed lines mentioned in [9]. Both transmission lines mentioned in the paper are 500 kV and have 8 sub-conductors in each phase. The orientation of the sub-conductors is different from the traditional one. In Fig. 3 and Fig. 4, we can see the orientations. HSIL-1's sub-conductors have a diameter of 20.93 mm. The sub-conductor with the greatest height from the ground is in the outside phases, at 32 m, while the one with the least height is in the central phase, at 24 m.

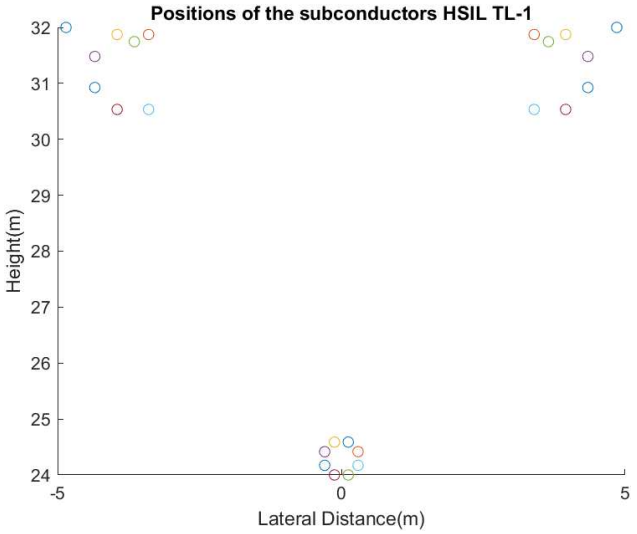

Fig. 3. Phase and sub-conductor's arrangement of the HSIL-1

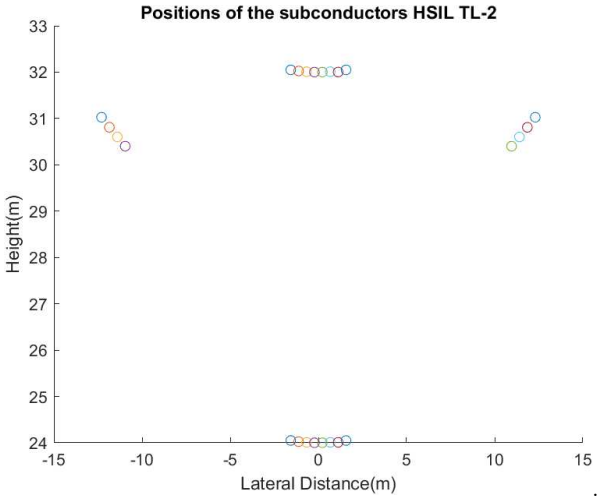

Fig. 4. Phase and bundle arrangement of the HSIL-2

This transmission line, like the previous one, has eight sub-conductors in each phase, and the properties of the sub-conductors are also like the previous one. For this design, the existing right of way (ROW) will be enough to implement.

To calculate the electric field for these two unconventional lines we must consider each sub-conductor separately. Because of its orientation, we cannot consider each bundle of sub-conductors as one conductor. That's why we must calculate the effect of 8×3=24 conductors with its image conductors. To do this we used the method discussed previously. The only difference between the conventional and the unconventional one is the consideration of radius while determining the potential coefficients. The mutual element of potential coefficient in Eq. (3) considers a real radius rather than the fictitious radius.

III. Results And Discussion

The previously described method is used to determine the electric field for the concerned transmission line (TL). In this paper two points are concerned to see the result; one is at ground level and the other is at 1 m above ground level. Fig.5 depicts the intensity of the electric field at ground level.

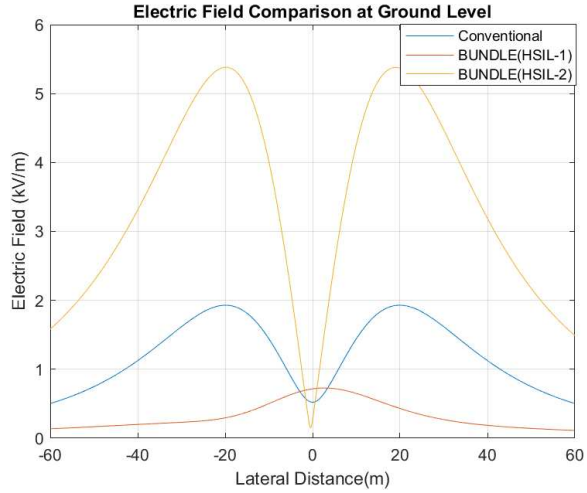

Fig. 5. Electric field under the TL at ground level.

In this graph, the blue line indicates the electric field due to the base case transmission line. One of the proposed transmission lines creates a lower amount of field than the base case transmission and the other creates a higher than the base case transmission line but both stay under the acceptable limit at the vicinity of the right of way.

Now another plot of electric field above the ground is given in Fig. 6. In this graph, it is shown like the previous one that the electric field is under the acceptable limit even 1 m above the ground.

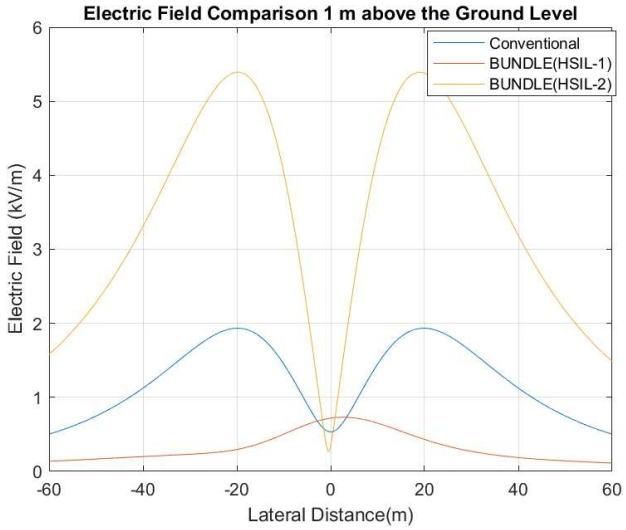

Fig. 6. Electric Field under the transmission lines at 1 m above the ground level.

Besides the electric field around these unconventional lines, the magnetic field around them, corona loss, radio and television noises, audible noise, live line working, etc. [10-18] should also studied about these lines towards their realization.

IV. Conclusion

This paper investigates techniques for calculating the intensity of electric field generated by overhead transmission lines. The proposed method employs multiple fictitious point charges for each sub-conductor. These methods allow for a more realistic depiction of bundle conductors while also eliminating the singularity problem in electric field intensity computations. The results of the calculations are compared to the base case findings along the lateral profile of a 500 kV overhead transmission line. The findings demonstrate that the proposed transmission line can be effectively employed in case of replacing the old one with the new unconventional line without violating acceptable limits and without creating new hazards to the vicinity of the right of way.

References

[1] E. Larson *et al.*, "Net-zero America: Potential pathways, infrastructure, and impacts," interim report, Princeton University, Princeton, NJ, 2020.

[2] MISO (Midcontinent Independent System Operator), *Transmission Cost Estimation Guide for MTEP23*, May 5, 2023.

[3] M. Ghassemi, "High surge impedance loading (HSIL) lines: A review identifying opportunities, challenges, and future research needs," IEEE Trans. Power Del., vol. 34, no. 5, pp. 1909–1924, Oct. 2019.

[4] J. Hernández, J. Segundo, P. Gomez, M. Borghei and M. Ghassemi, "Electromagnetic transient performance of optimally designed high surge

impedance loading lines," *IEEE Power & Energy Society General Meeting (PESGM)*, Montreal, QC, Canada, 2020, pp. 1–5

[5] M. Borghei and M. Ghassemi, "Future transmission lines with increased loadability through geometrical optimized phase configurations and sub-conductors in the bundle," *IEEE Power & Energy Society Innovative Smart Grid Technologies Conference (ISGT)*, Washington, DC, USA, 2020, pp. 1–5.

[6] M. Borghei and M. Ghassemi, "Geometrically optimized phase configurations and sub-conductors in the bundle for power transmission efficiency," *IEEE Electrical Insulation Conference (EIC)*, Calgary, AB, Canada, 2019, pp. 295-299.

[7] M. A. Khan and M. Ghassemi, "A new unusual bundle and phase arrangement for transmission line to achieve higher natural power," *North American Power Symposium (NAPS)*, Asheville, NC, USA, 2023, pp. 1-5.

[8] H. Wei-Gang, "Study on conductor configuration of 500-kV Chang-Fang compact line," *IEEE Trans. Power Del.*, vol. 18, no. 3, pp. 1002–1008, Jul. 2003.

[9] M. A. Khan and M. Ghassemi, "A new method for calculating electric field intensity on subconductors in unconventional high voltage, high power density transmission lines," *IEEE Conf. Electr. Insul. Dielectr. Phenomena (CEIDP)*, East Rutherford, NJ, USA, 2023.

[10] M. A. Khan and M. Ghassemi, "Corona loss calculation for unconventional high surge impedance loading transmission lines," *IEEE* North American Power Symp. (NAPS), Asheville, USA, 2023, pp. 1–6.

[11] M. A. Khan and M. Ghassemi, "Calculation of audible noise and radio interference for unconventional high surge impedance loading (HSIL) transmission lines," *IEEE Conf. Electr. Insul. Dielectr. Phenomena (CEIDP)*, East Rutherford, NJ, USA, 2023.

[12] E. Arafat, B. Porkar, and M. Ghassemi, "Magnetic field calculation under unconventional lines with increased power delivery," *IEEE Texas Power and Energy Conf. (TPEC)*, College Station, TX, USA, 2024.

[13] M. Ghassemi, M. Farzaneh, and W. A. Chisholm, "Three-dimensional FEM electrical field calculation for FRP hot stick during EHV live-line work," *IEEE Trans. Dielectr. Electr. Insul.*, vol. 21, no. 6, pp. 2531–2540, Dec. 2014.

[14] M. Ghassemi and M. Farzaneh, "Coupled computational fluid dynamics and heat transfer modeling of the effects of wind speed and direction on temperature increase of an ice-covered FRP live-line tool," *IEEE Trans. Power Del.*, vol. 30, no. 5, pp. 2268–2275, Oct. 2015.

[15] M. Ghassemi, M. Farzaneh, and W. A. Chisholm, "A coupled computational fluid dynamics and heat transfer model for accurate estimation of temperature increase of an ice-covered FRP live-line tool," *IEEE Trans. Dielectr. Electr. Insul.*, vol. 21, no. 6, pp. 2628–2633, Dec. 2014.

[16] M. Ghassemi and M. Farzaneh, "Calculation of minimum approach distances for tools for live-line working under freezing conditions," *IEEE Trans. Dielectr. Electr. Insul.*, vol. 23, no. 2, pp. 987–994, Apr. 2016.

[17] M. Ghassemi, "High surge impedance loading (HSIL) lines: A review identifying opportunities, challenges, and future research needs," *IEEE Trans. Power Del.*, vol. 34, no. 5, pp. 1909–1924, Oct. 2019.

[18] M. Ghassemi and M. Farzaneh, "Effects of tower, phase conductors and shield wires on the electrical field around a tower window during live-line work," *IEEE Trans. Dielectr. Electr. Insul.*, vol. 22, no. 6, pp. 3413–3420, Dec. 2015.